The Role of Hydrogen in Corrosion Fatigue of High Purity Al-Zn-Mg Exposed to Water Vapor

R. E. RICKER and D. J. DUQUETTE

Corrosion fatigue tests were performed on samples of a high purity Al-Zn-Mg alloy in humid nitrogen gas after pre-exposure to either vacuum or humid air. The results of these tests were compared to the results of fatigue tests performed in dry nitrogen, used as an inert reference environment, after the same pre-exposure treatments. The pre-exposure times were calculated by assuming that bulk diffusion of hydrogen was the rate limiting process in either hydrogen adsorption or desorption. Water vapor in the testing environment resulted in reduced fatigue lives; however, pre-exposure to humid air was just as detrimental as water vapor in the test environment. The pre-exposure embrittlement effect of humid air was found to be completely reversible when the samples were stored in a vacuum long enough to remove hydrogen, assuming a bulk diffusion coefficient of 1×10^{-13} m^2/sec. These results confirm the hypothesis that the reduced fatigue lives of Al-Zn-Mg alloys in water vapor is due to hydrogen embrittlement.

I. INTRODUCTION

ALUMINUM alloys, and in particular the high strength Al-Zn-Mg alloys, are susceptible to environmentally assisted crack growth. The first mechanistic models developed to explain stress corrosion cracking (SCC) of Al-Zn-Mg alloys were based on either stress assisted dissolution of the highly strained plastic zone at the crack tip or on passive film rupture and dissolution at active slip steps.[1,2] The localization of the crack path to the grain boundaries was thought to be due to either segregation of alloying elements or impurities to the grain boundaries or to preferential slip in the soft precipitate free zones.[1,2] Later, it was proposed that stress corrosion cracking could be caused by a hydrogen embrittlement process resulting from the cathodically evolved hydrogen which invariably accompanies the corrosion process on aluminum alloys.[3,4,5] Hydrogen gas bubble nucleation and growth at grain boundaries has been observed in the transmission electron microscope.[6] However, Ford[7,8] demonstrated that a calculation of anodic dissolution rates can quantitatively explain the observed crack growth rates, while hydrogen embrittlement, at least by the gas bubble nucleaton mechanism of Zapffe and Sims,[9] can not.

Studies on pre-exposure of Al-Zn-Mg alloys to environments containing water and water vapor have shown that the alloys are embrittled by exposure to either liquid or vapor phase water.[10–15] Tests have shown that there is a strong relationship between pre-exposure, test environment, strain rate, and ductility.[10–15] Holroyd and Hardie[15] tested an Al-Zn-Mg alloy [7049] in dry air at varying strain rates after a three day pre-exposure to seawater, and found a minimum in ductility at a strain rate of $1 \times 10^{-4m}/(m \cdot s)$. They attributed the minimum in ductility to increasing embrittlement with lower strain rates until the rate of hydrogen desorption during testing resulted in the loss of the embrittling species before failure.[15] They reported that storage of the samples in vaccuum was not effective in restoring the ductility and concluded that dislocation motion was required to remove hydrogen.[15] Swann *et al.*[16,17] found that pre-exposure to moist gases resulted in embrittlement and hydrogen absorption as detected by straining in a vacuum chamber equipped with a mass spectrometer.

In contrast to SCC where cracking is virtually always intergranular, transgranular cracking or mixed intergranular and transgranular cracking is usually observed for corrosion fatigue (CF) of aluminum alloys although the same mechanisms have been proposed to explain the role of the environment in the fracture process.[18–21] To distinguish between anodic dissolution and hydrogen embrittlement mechanisms in corrosion fatigue, Stoltz and Pelloux[22] studied the effect of electrochemical potential on crack growth rates of precracked samples of alloy 7075 and concluded that dissolution was responsible for the accelerated crack propagation. However, in a similar study on smooth samples of alloy 7075, Jacko and Duquette[23,24] showed that the fatigue lives of samples were reduced by the addition of a hydrogen recombination poison (As) and found that corrosion fatigue was reduced, but not eliminated, in torsional loading (Mode III). However, Ford[25] demonstrated that, as in the case for SCC, anodic dissolution is quantitatively capable of explaining the observed CF crack growth rates in an Al-7 pct Mg alloy.

Unambiguous distinction between anodic dissolution mechanisms and hydrogen embrittlement mechanisms is difficult for aluminum alloys exposed to aqueous solutions. Aluminum is an active metal ($E^\circ = -1.71$ V_{she}) and the Flade potential is active with respect to the hydrogen electrode.[26] As a result, hydrogen evolution accompanies dissolution even during anodic polarization.[26,27] Also, cathodic polarization results in the accumulation of hydroxyl ions at the surface which attack the passivating film causing dissolution of the metal.[28–31]. As a result, a test program was developed utilizing water vapor and an inert gaseous environment (dry nitrogen) to test the hypothesis that hydrogen in solid solution could accelerate fatigue failure of Al-Zn-Mg alloys.

II. THEORY

The chemical reactions which occur between water and aluminum metal to yield hydrous aluminum oxides and/or hydroxides can be represented by the following equation:

R. E. RICKER is Metallurgist, Institute for Materials Science and Engineering, National Bureau of Standards, Gaitherburg, MD 20899. D. J. DUQUETTE is professor, Department of Materials Engineering, Rensselaer Polytechnic Institute, Troy, NY 12181.

Manuscript submitted August 24, 1987.

$$2Al(s) + (3 + X)H_2O \rightarrow Al_2O_3 \cdot X(H_2O)\,(s) + 3H_2(g) \quad [1]$$

Where the degree of hydration of the resulting oxide (X) varies from 0 to 3. The different phases that form the corresponding degree of hydration are given in Table I.[32,33,34]

Scamans and Tuck[37] studied the reactions and the products that form when aluminum is exposed to water vapor at 70 °C. They found that exposure to water vapor resulted in the formation of a duplex film of pseudoboehmite ($X = 2$) and bayerite ($X = 3$). They also observed blistering of the film caused by the hydrogen gas evolved during the reactions. According to the thermodynamic information given in Table I, the equilibrium partial pressure of hydrogen for the formation of bayerite on aluminum at 87 pct relative humidity and 25 °C is greater than 10^{53} Pa (10^{48} atm) and greater than 10^{39} Pa (10^{34} atm) for the formation of boehmite. Also, at the interface between the bayerite and the aluminum metal the following reaction is possible:

$$2Al(s) + 6Al_2O_3 \cdot 3H_2O(\text{bayerite}) \rightarrow 4Al_2O_3(\text{corundum}) + 3H_2(g) \quad [2]$$

The standard free energy change for the formation of corundum by this reaction is −841.3 kJ/mole for which the equilibrium partial pressure of hydrogen is greater than 10^{54} Pa (10^{49} atm).[32,33,34]

Hydrogen evolution occurs rapidly and Scamans and Tuck[37] observed blistering of the surface oxide film within 15 seconds of exposure to water vapor and bayerite growth within 5 minutes of exposure. However, the rate of absorption of hydrogen will be limited by solid state diffusion of hydrogen into the metal. Extrapolation of hydrogen diffusion measurements made at elevated temperatures (450 to 625 °C) to 25 °C indicates that the diffusion constant for hydrogen in aluminum is between 10^{-12} and 10^{-14} m^2/sec.[35,36] Scamans and Tucks[37,38,39] and Gest and Troiano[10,11] have measured the diffusion of hydrogen in Al-Zn-Mg alloys at or near room temperature. Scamans and Tuck used water vapor saturated air (70 °C) as the hydrogen source in a permeation cell and found the hydrogen diffusion constant to be approximately 10^{-14} m^2/sec.[37,38,39] Gest and Troiano used aqueous solutions in an electrochemical permeation cell to estimate the hydrogen diffusion coefficient as 2×10^{-13} m^2/sec at 25 °C.[10,11] Since the rate determining step in hydrogen absorption is solid state diffusion of the dissolved hydrogen into the alloy, pre-exposure treatments intended to charge samples with hydrogen must allow sufficient time for solid state diffusion of hydrogen into the sample. Also, since aluminum samples can absorb hydrogen during fabrication or from laboratory air prior to testing, control samples must be purged of hydrogen prior to testing by a pre-exposure treatment to vacuum. The vacuum pre-treatment of the control samples must be for a time period which will allow solid state diffusion of the internal hydrogen to the surface where it can be desorbed.

There are four different ways that exposure and/or pre-exposure to water vapor can influence the fatigue resistance of Al-Zn-Mg alloys. These are:

1. Pre-Existing Internal Hydrogen: Solid state dissolved hydrogen present in the alloy prior to fatigue loading will be available to diffuse to the plastic zone ahead of a fatigue crack or to the surface and cause embrittlement.
2. Pre-Existing Corrosion Damage: During exposure to water vapor prior to fatigue loading, corrosion damage occurs. Also, the presence of a large hydrogen partial pressure in the metal could result in irreversible damage such as the nucleation of internal voids. The presence of this damage may contribute to the initation and propagation of fatigue cracks.
3. Oxidation Effects: Oxidation of aluminum metal and the growth of a brittle oxide film on the surface or at the crack tip could accelerate fatigue crack initiation and propagation (includes oxide induced closure effects).
4. Externally Generated Hydrogen: Hydrogen is generated at the surface and at a crack tip as a by product of the corrosion reaction between water vapor and unfilmed aluminum metal. Thus, rupture of the passive film by emerging slip steps at the crack tip will result in hydrogen production at the crack-tip. This hydrogen can be absorbed into the alloy and interact with the surface or plastic deformation to cause embrittlement.

Table I. The Oxide Phases of The Aluminum-Water System[32,33,34]
General Reaction: $2Al(s) + (3 + X)H_2O \rightarrow Al_2O_3 \cdot X(H_2O)\,(s) + 3H_2(g)$

Degree of Hydration (X)	Chemical Composition	Phases	ΔG (kJ/mol.)
0	anhydrous aluminum oxide Al_2O_3	corundum	−864.8
1	aluminum oxyhydroxide $Al_2O_3 \cdot H_2O$ or AlOOH	boehmite diaspore	−864.8 —
2	hydrated aluminum oxyhydroxide $Al_2O_3 \cdot 2(H_2O)$ or $AlOOH \cdot (H_2O)$	pseudoboehmite	—
3	tri-hydrated aluminum oxide $Al_2O_3 \cdot 3(H_2O)$	bayerite nordstrandite gibbsite (hydrargillite)	−888.3 — −897.2
3	aluminum hydroxide $2[Al(OH)_3]$	amourphous hydroxide	−852.0

The goal of this investigation was to evaluate the relative contributions of each of these factors individually and in combined action and, thereby, test the hydrogen embrittlement hypothesis. As a result, a test program with five different combinations of pre-exposure treatment and test environment was employed. These are:

A. Vacuum/Dry Nitrogen: Samples purged of hydrogen by a vacuum pre-exposure were tested in an inert environment as a standard reference fatigue life curve (no environmental contribution to failure).

B. Humid Air/Humid Nitrogen: Samples pre-corroded and pre-charged with hydrogen by pre-exposure to humid air were tested in a corrosive chemical environment to test the combined effect of all four of the possible mechanisms discussed above.

C. Vacuum/Humid Nitrogen: Samples purged of hydrogen by vacuum pre-exposure were tested in a corrosive (humid) environment that also provided hydrogen at the surface of the sample. For these samples, only mechanisms 3 and 4 can contribute to failure.

D. Humid Air/Dry Nitrogen: Samples pre-corroded (and thus pre-charged with hydrogen) were tested in an inert environment to test the effect that hydrogen in internal solid solution would have on the fatigue properties of this alloy. For these samples, only mechanisms 1 and 2 can contribute to fatigue failure.

E. Humid Air Then Vacuum Outgassed/Dry Nitrogen: Samples pre-corroded and pre-charged with hydrogen by a pre-exposure treatment to humid air were purged of hydrogen by a vacuum exposure and fatigue tested in an inert environment to test the effect of the pre-corrosion damage and to test the reversibility of the pre-exposure embrittlement effect (mechanism 2 only).

III. EXPERIMENTAL

Samples 80 mm long and 20 mm wide with a central gage section 10 mm wide and 13 mm long were machined from a sheet of high purity ternary Al-5.64 pct Zn-1.94 pct Mg alloy, solution treated in argon at 465 °C for an hour, quenched in cold water, and aged in silicon oil at 120 °C for 24 hours to achieve peak hardness.[29] This resulted in equiaxed grains with an average diameter of 0.127 mm (ASTM size 3).

The samples were ground in oil and in a kerosene/paraffin mixture to the equivalent of a 600 grit finish, cleaned, and electropolished in a perchloric acid/ethanol solution.[40] The resulting samples were approximately 1.0 mm thick. After electropolishing, the samples were stored either in a vacuum chamber, to remove hydrogen and to prevent hydrogen absorption, or in a 10 liter chamber where the relative humidity was held constant at 87 pct to charge the samples with hydrogen.[13, 37–39] A rotary vane oil sealed mechanical vacuum pump was used to evacuate the vacuum chamber and the humidity was maintained constant in the humidity chamber by including a beaker containing ~500 ml of saturated sodium carbonate solution (with excess solid) for which the equilibrium relative humidity at 25 °C is 87 pct.[41]

In Appendix 1, the rate of hydrogen absorption (or removal) is calculated for different hydrogen diffusion coefficients which encompass the values found in the literature for hydrogen in aluminum. Table II gives the percentage of the total hydrogen absorbed (or removed) for different exposure times and diffusion coefficients. Fatigue lives were found to be a function of pre-exposure times for pre-exposures of less than 30 days but not of longer exposures. Accordingly, this minimum exposure period was adopted for both the vacuum pre-exposure (to outgas hydrogen absorbed during sample preparation) and for the water vapor pre-exposure (to charge samples with hydrogen).

Table II. Exposure Time Required to Charge or Remove Hydrogen from the Samples for Different Diffusion Coefficients (Appendix)

Percentage Absorbed (M_t/M_∞) × 100 Pct	Exposure Time Required (Days) $D_H = 1 \times 10^{-12}$ (m²/sec)	$D_H = 1 \times 10^{-13}$ (m²/sec)	$D_H = 1 \times 10^{-14}$ (m²/sec)
99.5	5.87	58.7	587
96.0	3.52	35.2	352
89.0	2.35	23.5	235
70.2	1.17	11.7	117
50.8	0.59	5.9	59

D_H = hydrogen diffusion coefficient at 25 °C in (m²/sec)
M_t = amount of hydrogen absorbed in exposure time (t)
M_∞ = amount of hydrogen absorbed with infinite exposure time

The fatigue tests were conducted with a four point bending machine in a 1.4 liter plexiglass chamber at a frequency of 2.778 Hz. The environmental chamber was used to control the environment for all tests. The cyclic bending moment was applied to the sample such that the cracks propagated across the short dimension of the sample. To help preserve fractographic features, the bending moment was not reversed and the minimum bending moment during a load cycle was zero. The stroke was controlled and monitored with an LVDT and the load was monitored with a load cell. The maximum strain at the surface was calculated from the equation for deflection of elastic beams related to the measured geometry of each individual specimen.[29,42] The accuracy of the calculations was confirmed with strain gages prior to environmental testing.

The dry nitrogen environment was maintained by a continuous flow of pure nitrogen (<3 ppm water and <0.5 ppm oxygen) at 0.22 liters per minute through a cold trap immersed in a reservoir filled with solid CO_2. The humid nitrogen environment was maintained by bubbling nitrogen at the same rate through distilled water, and then through a solution of sodium carbonate saturated with excess solid to maintain the relative humidity at 87 pct (25 °C).[29,41]

The fracture surfaces were examined in a scanning electron microscope (SEM). To evaluate the relative influence of environment and stress intensity on the mode of fracture, lines were drawn on SEM micrographs perpendicular to the direction of crack propagation at three different crack depth to sample thickness ratios (0.25, 0.50, and 0.75). To minimize errors which may be introduced by edge effects and isolated initiation events, a length of line representing 25 pct of the width of the sample (2.5 mm) in the central region of the sample was used for this determination. The ratio of the length of this line which traversed intergranular fracture to the total length of line was taken as the percentage of intergranular fracture. Twelve measurements (four at each of three different crack lengths) were made for each testing environment. The stress intensity factors were estimated for each measurement using an asymptotic approximation for a thin strip with a single edge crack in bending assuming straight line crack geometry.[43] Variations in crack shape and

other factors will influence the actual stress intensity, and these rough estimates of the average stress intensity are included to illustrate the trend in the magnitude of the stress intensity with crack length.

IV. RESULTS

A. *Tests in Dry Nitrogen Gas after Vacuum Pre-Exposure*

Figure 1 shows the results of fatigue tests in dry nitrogen after a pre-exposure treatment to vacuum of 30 days or more. Reduced fatigue lives were found for vacuum pre-exposures of less than 30 days. As a result, only samples which were stored in a vacuum for longer than 30 days were used for this inert reference environment fatigue life curve. These data are used as a base-line comparison (best fatigue resistance) for subsequent tests.

B. *Tests in Humid Nitrogen after Pre-Exposure to Humid Air*

The results of corrosion fatigue tests performed in humid nitrogen after a pre-exposure treatment in humid air (>30 days at 87 pct R.H.) are also shown in Figure 1. For this testing condition, pre-existing internal hydrogen, pre-existing corrosion damage, oxidation effects, and externally generated hydrogen can contribute to reducing fatigue life. The results of these tests show that both the fatigue lives at a fixed strain range and the 10^6 cycles fatigue limit are significantly reduced by this combination of pre-exposure treatment and test environment.

C. *Tests in Humid Nitrogen after Pre-Exposure to Vacuum*

Two samples were tested in humid nitrogen without pre-exposure to humid air (vacuum pre-exposure) and compared to the aforementioned tests which should represent the maximum and minimum possible environmental influence of humid air (87 pct relative humidity). One sample was tested at a strain range of 0.004 m/m which is near the vacuum pre-exposure/dry nitrogen 10^6 cycles fatigue limit while the other was tested at a larger strain range. For this testing condition, there is neither pre-existing internal hydrogen dissolved in the sample nor corrosion damage on the surface of the sample at the onset of testing. As shown in Figure 2, the fatigue lives of these samples were essentially the same as that of samples pre-exposed to water vapor and tested in water vapor. This demonstrates that the pre-exposure treatment is not required to obtain the reduction in fatigue properties observed above.

D. *Tests in Dry Nitrogen after Pre-Exposure to Humid Air*

Fatigue tests were also conducted in dry nitrogen on samples which received the standard pre-exposure treatment to humid air. These samples contained internal solid state dissolved hydrogen and surface corrosion damage at the onset of testing as a result of the pre-exposure treatment. However, no hydrogen was available from the environment during the test and no corrosion processes could occur during the test which did not occur in the base-line reference environment tests. These data, shown in Figure 2, indicate that the fatigue lives of these samples were essentially identical to the fatigue lives of samples tested in humid nitrogen after pre-exposure to water vapor. The only deviation occurs near the fatigue limit where the duration of the test in dry nitrogen is such that significant hydrogen desorption may occur.

E. *Tests in Dry Nitrogen and Pre-Exposure to Humid Air and Vacuum*

To test the reversibility of the effect of pre-exposure to water vapor, tests were conducted in dry nitrogen on samples that were pre-exposed to humid air for more than a month and then placed in a vacuum for varying time periods. The vacuum exposure will remove the hydrogen absorbed into the alloy during the pre-exposure to humid air but, it will not remove the surface damage caused by corrosion during the humid air exposure. For samples placed in the vacuum for more than a month, the fatigue properties in dry nitrogen, also shown in Figure 2, were the same or better than those found for samples not exposed to humid air. That is, the fatigue properties were completely restored by the vacuum exposure or room temperature "bake out". To examine the rate of this recovery, tests conducted after various storage times

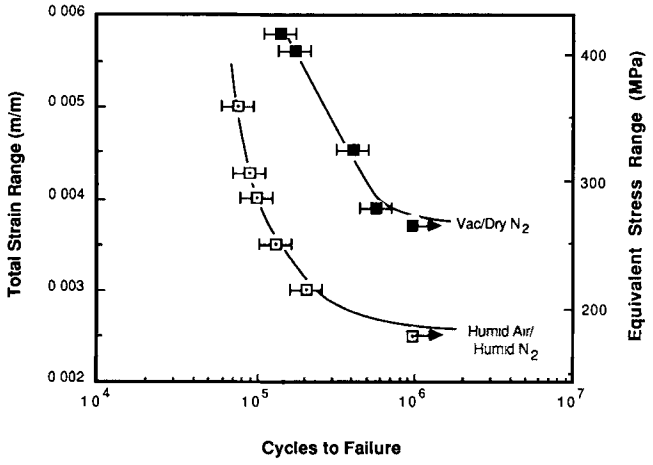

Fig. 1 — Cycles to failure for vacuum outgassed samples tested in dry nitrogen gas and for samples pre-exposed to humid air tested in humid nitrogen gas. Each point represents a single test and the error bars represent a two standard deviation range of the error as determined by regression analysis.

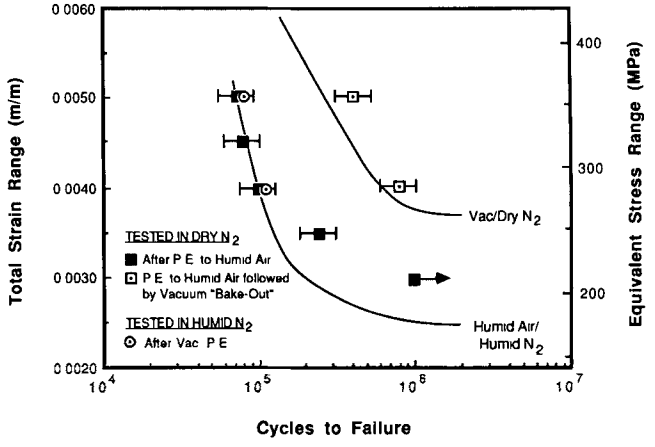

Fig. 2 — The effect of different pre-exposure and test environment combinations on fatigue life as compared to the results shown in Figure 1 for vacuum outgassed samples tested in dry nitrogen gas and for samples pre-exposed to humid air and tested in humid nitrogen gas. Each point represents a single test and the error bars represent a two standard deviation range of the error as determined by regression analysis.

in the vacuum were plotted as a percent of recovered fatigue life (on the logarithmic scale) *vs* the exposure time, as shown in Figure 3. Also, shown on this graph is the percentage of hydrogen that would be desorbed for different effective hydrogen diffusivities (Appendix 1). From this, it can be seen that the rate of recovery corresponds to the rate at which hydrogen would desorb from the sample assuming an effective diffusion coefficient of 1×10^{-13} m^2/sec.

F. *Fractography*

The fracture surfaces were examined in the SEM and regions of intergranular and transgranular crack propagation were observed on all samples. The percentage of intergranular fracture in the testing environments was determined by linear intercept at constant crack length on SEM fractographs. The average percentage of intergranular fracture for each environment is plotted against the crack length to thickness (a/h) ratio in Figure 4. In this figure, each point represents the average of four measurements, the error bars represent the standard deviation of the measurements, and the lines through the points are the regression lines determined from the measurements. The stress intensities were estimated for each sample and crack length to thickness (a/h) ratio, assuming simple straight line crack geometry. The averages of these values are included in Figure 4 to show how the stress intensity can be expected to vary with the (a/h) ratio. In this figure, it can be seen that the percentage of intergranular fracture at each (a/h) ratio was lower in dry nitrogen gas than in humid nitrogen gas. In dry nitrogen gas, the percentage of intergranular fracture did not change significantly with increasing cyclic stress intensity while in humid nitrogen it increased significantly. The regression lines indicate that the percentage of intergranular fracture is not significantly different for short crack lengths and, as this figure implies, crack initiation was primarily transgranular occurring at persistent slip bands.

Figures 5 through 10 are scanning electron micrographs of typical fracture surfaces, and in these figures the macroscopic direction of crack propagation is from the bottom of the figure to the top. A typical region of the transgranular crack propagation observed in dry nitrogen gas is shown in

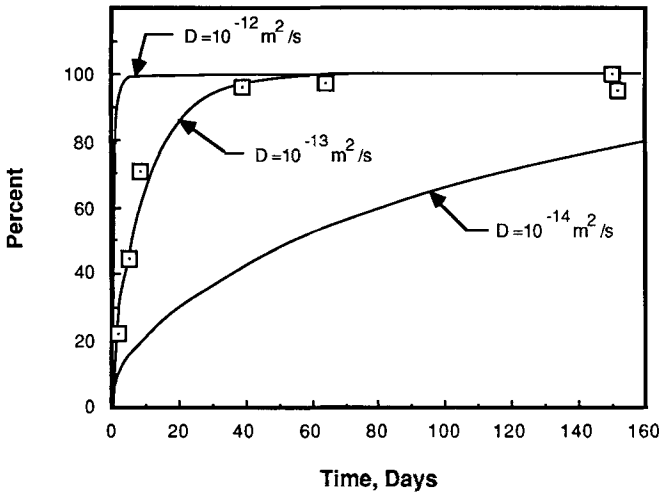

Fig. 3—Comparison of the rate of fatigue life recovery to the calculated percent of the hydrogen content which would be desorbed for different hydrogen diffusion coefficients.

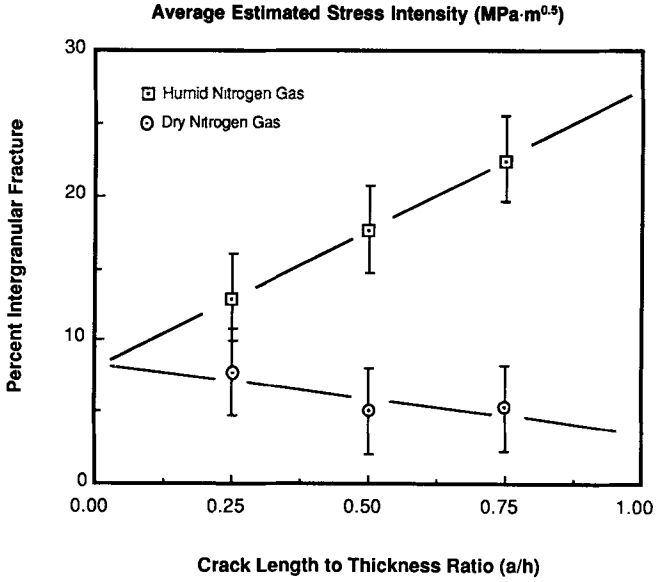

Fig. 4—The percentage of intergranular fracture determined by linear intercept at constant crack length *vs* crack length and average estimated stress intensity.

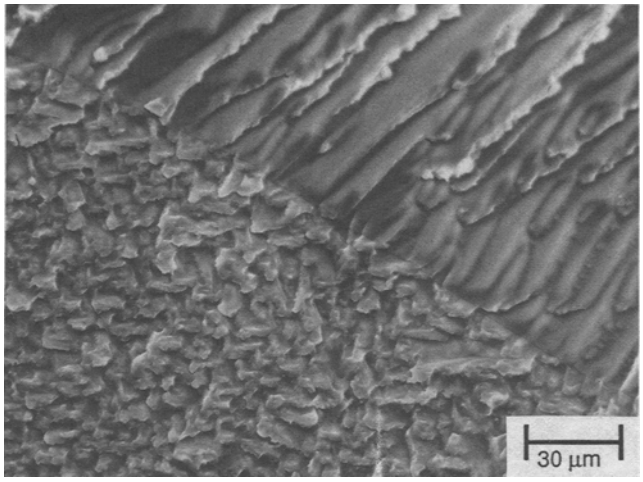

Fig. 5—The transgranular cleavage-like crack propagation in two grains of a vacuum outgassed sample tested in dry nitrogen gas.

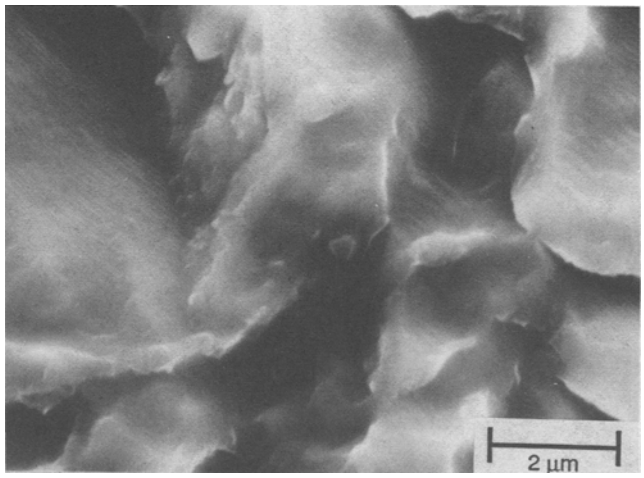

Fig. 6—A region of small transgranular cleavage-like facets on the fracture surface of a vacuum outgassed sample tested in dry nitrogen gas.

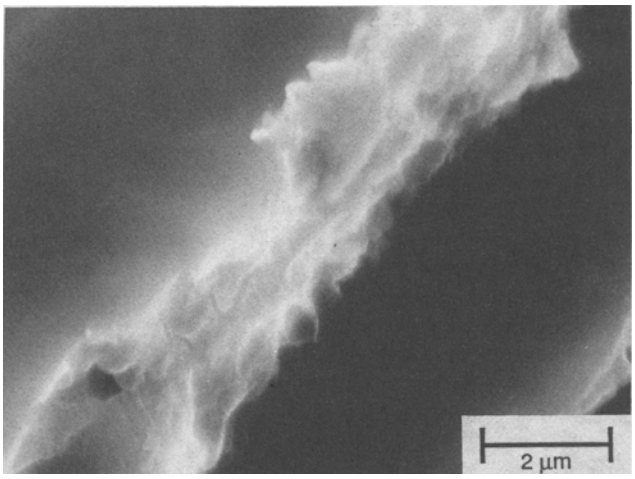

Fig. 7 — The face of the step between two facets of transgranular cleavage-like fracture on the fracture surface of a vacuum outgassed sample tested in dry nitrogen gas.

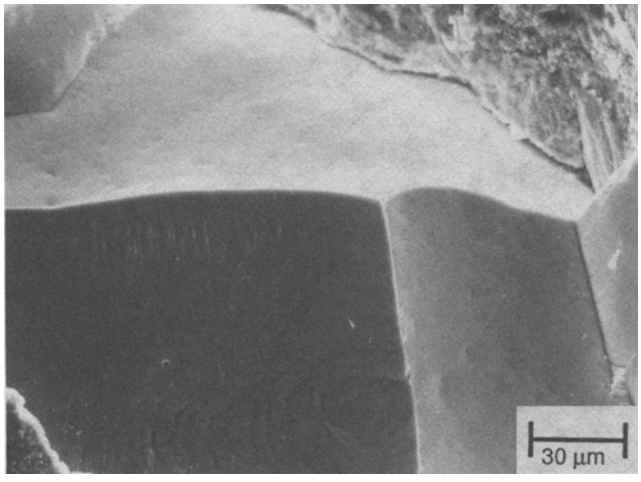

Fig. 8 — A region of intergranular crack propagation in a vacuum outgassed sample tested in dry nitrogen gas.

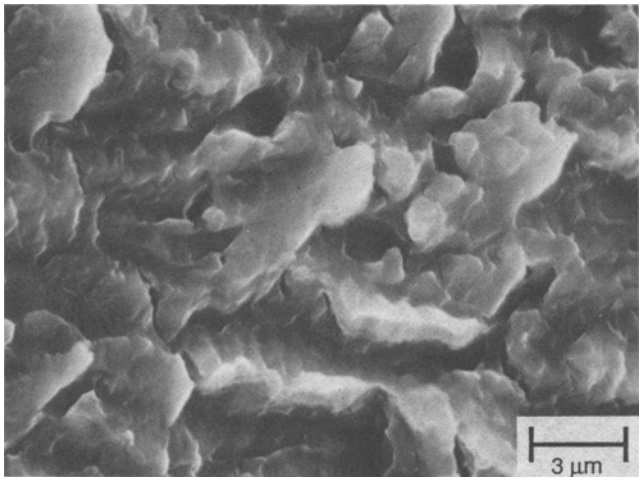

Fig. 9 — A region of transgranular crack propagation in a sample tested in humid nitrogen gas.

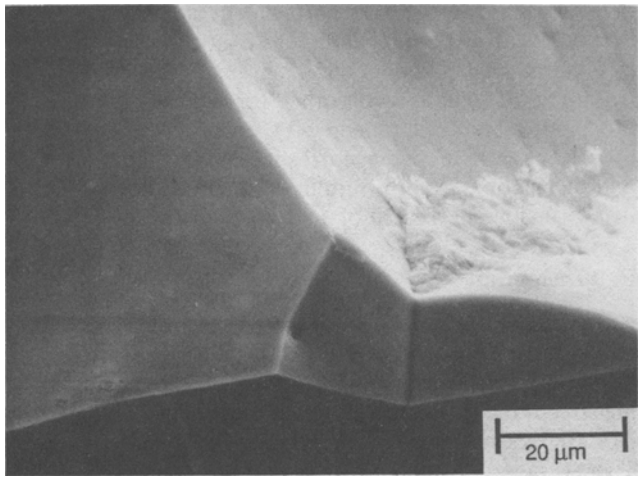

Fig. 10 — A region of intergranular crack propagation in a sample tested in humid nitrogen gas.

Figure 5. In this figure, the crack propagated across a grain oriented favorably for the formation of small cleavage-like facets into a grain oriented for the formation of larger facets. The region of small facets is shown at a higher magnification in Figure 6 and striations can be seen on the fracture surface. These striations are approximately 0.1 μm apart, indicating a crack growth rate of 1×10^{-7} meters/cycle. The face of a step between two regions of cleavage-like fracture is shown in Figure 7. Evidence of ductile deformation and corrosion can be seen on this surface. The corrosion may have occurred after testing, but the nitrogen environment is not completely oxygen free (<0.5 ppm oxygen) and fretting corrosion of this surface may have obscured the features on this surface, indicative of the actual fracture mechanism. Typically, the intergranular fracture surfaces formed in this environment were smooth and almost featureless, as shown in the upper half of Figure 8. The features shown on the grain boundary in the lower left of this figure were not observed on any other grain boundary.

Testing in humid nitrogen resulted in a slight increase in the percentage of intergranular fracture, especially at longer crack lengths. The transgranular cleavage-like fracture observed in this environment is shown in Figure 9. The surfaces appear flat and smooth, indicating that little plastic deformation is associated with crack propagation. The intergranular fracture surfaces of samples tested in this environment appeared similar to the intergranular fracture surfaces produced in dry nitrogen. Figure 10 shows an intergranular fracture surface formed in humid nitrogen and, except for some corrosion damage, it does not appear significantly different from that shown in the upper half of Figure 8. The external surface of a sample tested in humid nitrogen is shown in Figure 11. This figure shows the blistering and cracking of the surface film that resulted from the combined action of cyclic loading and water vapor.

V. DISCUSSION

In the theory section of this paper, it was pointed out that there are four different ways that exposure or pre-exposure to water vapor can accelerate fatigue failure. These are:

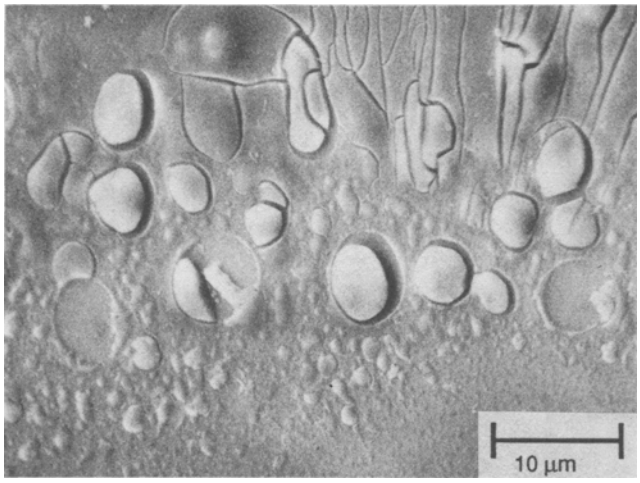

Fig. 11—Blistering and cracking of the external electropolished surface of a sample after exposure to humid air and cyclic loading in humid nitrogen gas.

1. pre-existing internal hydrogen,
2. pre-existing corrosion damage,
3. oxidation effects, and
4. externally generated hydrogen.

Corrosion damage generated during pre-exposure to water vapor cannot be removed by a simple vacuum exposure at room temperature, while the present results show that a vacuum exposure can result in complete recovery of fatigue resistance. Therefore, surface damage due to pre-exposure to water vapor cannot be responsible for the observed loss in fatigue resistance. Oxidation effects, such as oxide induced closure, would be environment dependent rather than pre-exposure dependent. Scamans and Tuck[37] showed that the kinetics of water vapor adsorption and hydrogen evolution are fast compared to bulk diffusion of hydrogen. Similarly, the kinetics of water vapor desorption from the surface will be fast with respect to bulk hydrogen diffusion. Also, Scamans and Tuck[37,38,39] demonstrated that exposure to water vapor results in hydrogen evolution, absorption, and diffusion into the metal. The results of the present study demonstrate that exposure to water vapor reduces the fatigue resistance of this alloy, that pre-exposure to water vapor is as damaging as water vapor in the testing environment, that the effect of water vapor is completely reversible, that the rate of recovery of the pre-exposure effect is slow requiring several days of vacuum exposure, and that the rate of recovery is exactly that predicted by hydrogen desorption kinetics for this sample geometry. There is no mechanism other than hydrogen embrittlement that can explain these observations. Also, since the same fatigue life results from pre-exposure to water vapor as results from water vapor in the testing environment, hydrogen present in the alloy at the onset of testing must be as effective in reducing the fatigue life as corrosion damage and hydrogen generation during the test.

Hydrogen may reduce the fatigue resistance of Al-Zn-Mg alloys by either surface adsorption at the crack tip or by embrittling the plastic zone ahead of the crack. Surface adsorption and interactions could reduce fatigue lives by reducing the surface energy and either reducing the energy required for brittle fracture as suggested by Uhlig,[44] or by increasing the number and activity of dislocation sources promoting shear at the crack tip as proposed by Lynch.[45] To embrittle the plastic zone ahead of the crack tip, water vapor would react with the bare metal surfaces exposed at the crack tip, producing significant amounts of mobile hydrogen atoms which then diffuse into the plastic zone ahead of the growing cracks accelerating fatigue crack growth by some internal hydrogen embrittlement mechanism. For the case of an alloy which is saturated with hydrogen and subsequently tested in a dry environment, the plastic zone ahead of the crack tip would be expected to act as a sink for hydrogen, since the hydrogen solubility would be higher in the crack tip process zone.[46]

The results of these experiments support the concept that hydrogen dissolved in the plastic zone and not surface adsorbed hydrogen is responsible for embrittlement. The rates of surface reactions and adsorption are much faster than the rate of bulk diffusion. As a result, if hydrogen adsorbed on the surface were responsible for embrittlement, then the fatigue lives of hydrogen pre-charged samples would not be identical to the fatigue lives of hydrogen free samples tested in humid nitrogen. However, if embrittlement occurs by an internal embrittlement process, then bulk diffusion from the surface or from the interior to the process zone would occur at about the same rate. Also, if adsorbed hydrogen, either produced by surface reactions or diffusing from the bulk to the crack surfaces, were responsible for the embrittlement phenomenon, then the correlation between the calculated amount of hydrogen desorbed and the embrittlement "recovery" process would not be observed. Rather, since adsorption is required only at the crack tip for it to be effective, then residual hydrogen in the alloy would saturate the surface and cause embrittlement for much longer out-gassing times then those predicted and observed in this investigation. On the other hand, a reduction in the general concentration of hydrogen in the alloy would be expected to reduce embrittlement if it occurs within the crack tip process zone by some internal embrittlement mechanism. Finally, the increasing deviation between the fatigue lives of pre-charged samples and samples tested in humid nitrogen with increasing testing time (Figure 2) can be explained by bulk diffusion reducing the hydrogen concentration in the sample while the opposite trend would be observed if bulk diffusion to the surface were a requirement for accelerated fatigue failure.

A model of internal rather than surface embrittlement is also supported by the fatigue experiments of Holroyd and Hardie[47] which showed that environmentally associated fatigue crack growth in aluminum alloy 7017-T651 is highly frequency dependent and related to the square root of time available during each cycle for crack propagation. A strong frequency dependence is not consistent with a surface adsorption phenomenon since the kinetics of adsorption on freshly produced crack surfaces should be virtually instantaneous. On the other hand, if there is no contribution of static load stress corrosion cracking during each load cycle, then as the frequency decreases the plastic zone ahead of the crack tip will become saturated with hydrogen and the crack propagation rate per cycle will approach a constant value. Wei *et al.*[48] studied the corrosion fatigue crack propagation rates of aluminum alloy 2219-T851 in water vapor and found that there was a critical frequency below which crack propagation was independent of frequency; however, they attributed this effect to mass transport up the crack.

The present study does not provide direct evidence for any specific mechanism of internal hydrogen embrittlement. The mixed intergranular and transgranular cracking observed in this study indicates that there is no unique fracture morphology associated with the mechanism or mechanisms of hydrogen assisted fracture. That is, it was found that hydrogen increased the percentage of intergranular fracture; however, this type of fracture was observed in the absence of damaging hydrogen species. Also, while hydrogen influenced the appearance of the transgranular fracture surfaces, this fracture mode was observed even with significant amounts of hydrogen dissolved in the alloy. In fact, Albrecht *et al.*[12] found that cathodic pre-charging 7075 tensile samples reduced the ductility and increased the size of the dimples observed on the fracture surfaces. These observations indicate that neither the chemistry nor the morphology of grain boundary/precipitate interactions is critical to environmental cracking. For example, it had been suggested that chemical differences between the grain boundary precipitates and the precipitate free zone (PFZ) might lead to galvanic corrosion of the grain boundary region [49–52] or to hydrogen embrittlement.[53,54] Alternatively, it has been suggested that the particular morphology of the grain boundary precipitates is required for crack propagation.[24–26,55] While both of these factors may influence the crack path and/or crack growth rates, apparently, they are not required for environmentally assisted cracking.

The fracture path appears to be determined by a variety of factors including the hydrogen concentration, the orientation or availability of a preferred path, and the loading conditions. Examination of the fracture surface revealed that frequently crack propagation was intergranular when small grains provided a convenient intergranular path. Stoltz and Pelloux[22] studied the effect of reducing grain size on corrosion fatigue resistance of alloy 7075 and they found that reducing grain size promoted intergranular fracture and increased crack propagation rates. This effect may be the result of hydrogen segregation to this region, the higher diffusivity of the grain boundary as compared to the matrix or simply the orientation of the grain boundary with respect to the stress distribution at the crack tip. Grain boundary separation in the presence of solid solution hydrogen has been observed in the transmission electron microscope to occur along non-coherent precipitate matrix interfaces with little or no accompanying plastic deformation.[6,47] The precipitate-matrix interfaces within the grains could also influence hydrogen segregation and fracture in a manner similar to the grain boundary precipitates. This would result in lowering the transgranular fracture resistance of this alloy in the presence of hydrogen more than that of other aluminum alloys which are not precipitation hardened or which are not hardened with precipitate phases with the same level of coherency strains between the matrix and the precipitate.

VI. CONCLUSIONS

It has been shown that the fatigue resistance of a high purity Al-Zn-Mg alloy is significantly reduced by the presence of water vapor in the testing environment. Also, an equivalent reduction in fatigue life was observed in dry nitrogen for samples pre-exposed to water vapor long enough for bulk diffusion to saturate the sample with hydrogen. When the samples that were pre-exposed to water vapor were stored in a vacuum, complete recovery of fatigue strength resulted and the rate of this recovery corresponded to the estimated rate of hydrogen desorption for a diffusion coefficient of 1×10^{-13} m^2/sec. These results can only be explained by a bulk hydrogen embrittlement mechanism. Therefore, we conclude that the reduction of the fatigue resistance of this alloy in water vapor is due to a form of hydrogen embrittlement.

APPENDIX

For the absorption or desorption of a species from a plane sheet where the surface concentration is not in equilibrium with the atmosphere, the surface boundary condition is:[56]

$$-D\left(\frac{\partial C}{\partial x}\right) = \alpha(C_0 - C_s) \qquad [A1]$$

Where C_0 is the surface concentration of the species in equilibrium with the atmosphere at infinite time, C_s is the actual surface concentration as a function of time and α is a proportionality constant. For a thin sheet ($-\lambda \leq X \leq \lambda$) initially at a uniform concentration C_2 and the exchange defined by Eq. [A1] for both surfaces, the solution for the concentration as a function of time (t) and position (X) is:[56]

$$\frac{C(X,t) - C_2}{C_0 - C_2} = 1 - \sum_{n=1}^{\infty} \frac{2L^2 \cos\left(\frac{\beta_n X}{\lambda}\right) \exp\left(\frac{-\beta_n^2 Dt}{\lambda^2}\right)}{(\beta_n^2 + L^2 + L)\cos\beta_n} \qquad [A2]$$

Where the β_n terms are the positive roots of the equation:

$$\beta \tan\beta = L = \left(\frac{\lambda\alpha}{D}\right) \qquad [A3]$$

The total amount of substance, M_t, entering or leaving the sheet up to time t is determined as a fraction of the total quantity that will be absorbed or desorbed to reach equilibrium at infinite time, M_∞, by the relationship:[56]

$$\frac{M_t}{M_\infty} = 1 - \sum_{n=1}^{\infty} \frac{2L^2 \exp\left(\frac{-\beta_n Dt}{\lambda^2}\right)}{\beta_n^2(\beta_n^2 + L^2 + L)} \qquad [A4]$$

For small values of the diffusion coefficient, the β_n terms can be approximated by the terms for the argument approaching infinity which for the first and second terms are:

$$\beta_1 = 1.5708 \qquad \beta_2 = 4.7124 \qquad [A5]$$

This approximation is good for values of the dimensionless parameter L greater than 10^2. From this, it can be seen that the second and higher order terms are small compared to the first term of the series and that a first term approximation will be good for all but short times. The first term approximation for this relationship is:

$$\frac{M_t}{M_\infty} = 1 - (0.81057)\left[\frac{L^2}{(2.467 + L^2 + L)}\right] \cdot \exp\left[-2.467\left(\frac{Dt}{\lambda^2}\right)\right] \qquad [A6]$$

For hydrogen in aluminum, diffusivities between 10^{-12} and 10^{-14} m^2/sec are expected.[35–39] As a result, the dimension-

less parameter, L, will be small compared to β_n^2 or L and Eq. [A6] can be approximated further as:

$$\frac{M_t}{M_\infty} = 1 - (0.81057)\exp\left[-2.467\left(\frac{Dt}{\lambda^2}\right)\right] \quad [A7]$$

This is equivalent to assuming that the surface reactions are fast compared to the rate of bulk diffusion. An equivalent relationship would be derived if this was assumed initially, but the validity of this assumption would not be as obvious.

The relationship of Eq. [A7] gives the amount of diffusing species (hydrogen) which will enter or exit the two sides of a plane sheet in time (t) as a fraction of the total that must enter or leave the sample to reach equilibrium with the environment ($t \rightarrow \infty$). From this relationship, the pre-exposure time required to charge a sample with a homogeneous (equilibrium) hydrogen distribution can be calculated which is equivalent to the time required to remove this same hydrogen concentration in a vacuum. Table II is a listing of the times required to charge or bake-out an aluminum sheet assuming different diffusion coefficients in the range found in the literature and for the sample geometry used in this study.[10,11,37-39]

ACKNOWLEDGMENTS

The authors are grateful for the support of this work by the United States Office of Naval Research under contract no. N00014-75-C-0466. Also, the authors would like to acknowledge the assistance of J. L. Fink and M. R. Fulcher.

REFERENCES

1. E. H. Dix, Jr.: *Trans. ASM*, 1950, vol. 42, pp. 1057-1127.
2. A. J. Sedriks, P. W. Slattery, and E. N. Pugh: *Trans. ASM*, 1969, vol. 62, pp. 815-18.
3. W. Gruhl and D. Brungs: *Metall.*, 1969, vol. 23, pp. 1020-26.
4. M. O. Speidel: *Hydrogen in Metals*, I. M. Bernstein and A. W. Thompson, eds., ASM, Metals Park, OH, 1974, pp. 249-76.
5. M. O. Speidel: *Metall. Trans. A*, 1975, vol. 6A, pp. 631-50.
6. L. Christodoulou and H. M. Flower: *Acta Metall.*, 1980, vol. 28, pp. 481-87.
7. F. P. Ford: *Met. Sci.*, 1978, vol. 12, pp. 326-34.
8. F. P. Ford, G. T. Burstein, and T. P. Hoar: *J. Electrochem. Soc.*, 1980, vol. 127, no. 6, pp. 1325-31.
9. C. Zapffe and C. Sims: *Trans. AIME*, 1941, vol. 145, pp. 225-71.
10. R. J. Gest and A. R. Troiano: *Corrosion*, 1974, vol. 30, no. 8, pp. 274-79.
11. R. Gest: Ph.D. Dissertation, Case Western Reserve University, Cleveland, OH, 1972.
12. J. Albrecht, A. W. Thompson, and I. M. Bernstein: *Metall. Trans. A*, 1979, vol. 10A, pp. 1759-66.
13. S. W. Ciaraldi: Ph.D. Dissertation, Univ. of Illinois at Urbana, Urbana, IL, 1980.
14. D. Hardie, N. J. H. Holroyd, and R. N. Parkins: *Met. Sci.*, 1979, vol. 13, pp. 603-10.
15. N. J. H. Holroyd and D. Hardie: *Corro. Sci.*, 1981, vol. 21, pp. 129-44.
16. L. Montgrain and P. R. Swann: *Hydrogen in Metals*, I. M. Bernstein and A. W. Thompson, eds., ASM, Metals Park, OH, 1974, pp. 575-84.
17. G. M. Scamans, R. Alani, and P. R. Swann: *Corro. Sci.*, 1976, vol. 16, pp. 443-59.
18. F. J. Bradshaw and C. Wheeler: *Intl. J. of Fract. Mech.*, 1969, vol. 5, no. 4, pp. 255-68.
19. T. Broom and A. Nicholson: *J. Inst. of Metals*, 1960-61, vol. 89, pp. 183-90.
20. C. A. Stubbington and P. J. E. Forsyth: *J. Inst. of Metals*, 1961-62, vol. 90, pp. 347-54.
21. C. A. Stubbington: *Metallurgia*, 1963, vol. 65, pp. 109-21.
22. R. E. Stoltz and R. M. Pelloux: *Metall. Trans.*, 1972, vol. 3, pp. 2433-41.
23. R. J. Jacko and D. J. Duquette: *Hydrogen Effects in Metals*, I. M. Bernstein and A. W. Thompson, eds., AIME, New York, NY, 1981, pp. 477-84.
24. R. J. Jacko and D. J. Duquette: *Metall. Trans. A*, 1977, vol. 8A, pp. 1821-27.
25. F. P. Ford: *Corrosion*, 1979, vol. 35, no. 7, pp. 281-87.
26. H. H. Uhlig: *Corrosion and Corrosion Control*, John Wiley and Sons, Inc., New York, NY, 1971.
27. C. B. Bargeron and R. C. Benson: *J. Elchem. Soc.*, 1980, vol. 127, no. 11, pp. 2528-30.
28. T. F. Klimowicz and R. M. Latanision: *Metall. Trans. A*, 1978, vol. 9A, pp. 597-99.
29. R. E. Ricker: *Corrosion Fatigue of an Al-Zn-Mg Alloy and an Al-Mg-Li Alloy*, Ph.D. Dissertation, Rensselaer Polytechnic Institute, Troy, NY, 1983.
30. R. E. Ricker and D. J. Duquette: Corro/85, Paper No. 354, NACE, Houston, TX, 1985.
31. T. H. Nguyen, B. F. Brown, and R. T. Foley: *Corro.*, 1982, vol. 38, no. 6, pp. 319-26.
32. R. S. Alwitt: *Oxides and Oxide Films*, J. W. Diggle and A. K. Vijh, eds., Marcel Dekker, Inc., New York, NY, 1976, vol. 4, pp. 169-254.
33. M. Pourbaix: *Atlas of Electrochemical Equilibrium Diagrams*, National Association of Corrosion Engrs., Houston, TX, 1974.
34. W. Vedder and D. A. Vermilya: *Trans. Faraday Soc.*, 1969, vol. 65, no. 554, p. 561.
35. K. Papp and E. Kovacs-Csentenyi: *Scripta Metall.*, 1981, vol. 15, pp. 161-64.
36. R. A. Outlaw, D. T. Peterson, and F. A. Schmidt: *Scripta Metall.*, 1982, vol. 16, pp. 287-92.
37. G. M. Scamans and C. D. S. Tuck: *Environment-Sensitive Fracture of Engineering Materials*, Z. A. Foroulis, ed., TMS-AIME, New York, NY, 1979, pp. 464-83.
38. G. M. Scamans and C. D. S. Tuck: *Mechanisms of Environment Sensitive Cracking of Materials*, P. R. Swann, F. P. Ford, and A. R. C. Westwood, eds., The Metals Soc., London, 1977, pp. 482-91.
39. C. D. S. Tuck and G. M. Scamans: *2nd Int. Congress on H in Metals*, 4A11, 1977, pp. 1-8.
40. C. A. Johnson: *Metallography Principles and Procedures*, Leco Corporation, St. Joseph, MI, 1977.
41. R. E. Bolz and G. L. Tuve: *Handbook of Tables for Applied Engineering Science*, 2nd ed., CRC Press, Cleveland, OH, 1973, p. 548.
42. E. P. Popov: *Introduction to Mechanics of Solids*, Prentice-Hall, Inc., Englewood Cliffs, NJ, 1968.
43. J. P. Benthem and W. T. Koiter: *Mechanics of Fracture I Methods of Analysis and Solutions of Crack Problems*, G. C. Shih, ed., Noordhoff Intl. Publ., Leyden, The Netherlands, 1973, pp. 131-78.
44. H. H. Uhlig: *Physical Metallurgy of Stress Corrosion Fracture*, T. N. Rhodin, ed., Interscience Publ., New York, NY, 1959, pp. 1-28.
45. S. P. Lynch: *Hydrogen Effects in Metals*, A. W. Thompson and I. M. Bernstein, eds., TMS-AIME, New York, NY, 1981, pp. 863-72.
46. C. F. Barth and E. A. Steigerwald: *Metall. Trans.*, 1970, vol. 1, pp. 3451-55.
47. N. J. Holroyd and D. Hardie: *Corro. Sci.*, 1983, vol. 23, no. 6, pp. 527-46.
48. R. P. Wei, P. S. Pao, R. G. Hart, T. W. Weir, and G. W. Simmons: *Metall. Trans. A*, 1980, vol. 11A, pp. 151-58.
49. A. J. Sedriks, J. A. S. Green, and D. L. Novak: *Metall. Trans.*, 1973, vol. 4, pp. 1992-94.
50. A. J. Sedriks, J. A. S. Green, and D. L. Novak: *Localized Corrosion*, NACE-3, Natl. Assn. of Corro. Engrs., 1974, pp. 569-75.
51. C. R. Shastry, M. Levy, and A. Joshi: *Corrosion Science*, 1981, vol. 21, no. 9, pp. 673-88.
52. A. Garner and D. Tromans: *Corrosion*, 1979, vol. 35, no. 3, pp. 55-60.
53. R. K. Viswanadham, T. S. Sun, and J. A. S. Green: *Corrosion*, 1980, vol. 36, no. 6, pp. 275-78.
54. R. K. Viswanadham, T. S. Sun, and J. A. S. Green: *Metall. Trans. A*, 1980, vol. 11A, pp. 85-89.
55. G. M. Scamans: *Journal of Matl. Science*, 1978, vol. 13, pp. 27-36.
56. J. Crank: *The Mathematics of Diffusion*, Clarendon Press, Oxford, England, 1975.